IOP FTC
IOP PUBLISHING JOURNAL OF PHYSICS A: MATHEMATICAL AND THEORETICAL
J. Phys. A: Math. Theor. **40** (2007) F185–F192 doi:10.1088/1751-8113/40/8/F01

**FAST TRACK COMMUNICATION**

# Vortex-free complex landscapes and umbilic-free real landscapes

**M V Berry**

H H Wills Physics Laboratory, Tyndall Avenue, Bristol BS8 1TL, UK

Received 7 December 2006, in final form 9 January 2007
Published 6 February 2007
Online at stacks.iop.org/JPhysA/40/F185

**Abstract**
Although complex scalar functions, varying over the infinite plane $\boldsymbol{r} = \{x, y\}$, commonly possess vortices (points of phase singularity), it is possible to devise exceptional functions with no vortices. Similarly, although real scalar functions representing surfaces as small departures from the plane commonly possess umbilic (locally spherical) points, it is possible to devise exceptional functions that do not possess them. Examples of both are given.

PACS number: 02.40.Xx

## 1. Introduction

Recent decades have seen renewed studies of singularities, motivated largely by applications in classical optics [1–3]. In particular, for smooth undulating functions in the plane $\boldsymbol{r} = \{x, y\}$, with zero mean (landscapes), attention has concentrated on two types of singularity. First are vortices (also called phase singularities or wave dislocations [4]), where a complex scalar function $\psi(\boldsymbol{r})$ vanishes. Second are umbilics [5, 6], which are points of equal principal curvatures, that is locally spherical points, of a landscape whose height above the $\boldsymbol{r}$ plane is represented by a real scalar function $h(\boldsymbol{r})$.

These singularities are ubiquitous. In isotropic Gaussian random landscapes, for example (superpositions of plane waves with different wavevectors $\boldsymbol{k}$), the density of vortices is [7]

$$d_{\mathrm{v}} = \frac{\langle k^2 \rangle}{4\pi}, \tag{1}$$

where the average is over the power spectrum of wavenumbers $k = |\boldsymbol{k}|$, and for umbilics the density is [6]

$$d_{\mathrm{u}} = \frac{\langle k^6 \rangle}{4\pi \langle k^4 \rangle}. \tag{2}$$

Roughly speaking, there are $\pi$ singularities per square mean wavelength.

The question addressed here is whether there exist exceptional landscapes with no singularities: complex landscapes with no vortices, and real landscapes with no umbilics.

  

Such landscapes can be constructed, as is shown by explicit examples in sections 2 (vortices) and 3 (umbilics). To avoid confusion, I should explain that my motivation is not that these landscapes are likely to find application (for example in experiments with optical beams), but simply to establish that they can exist.

## 2. Vortices

In terms of modulus $\rho$ and phase $\chi$, and real and imaginary parts $\xi$ and $\eta$, the vortices $\rho = 0$ in a complex scalar landscape

$$\psi(\boldsymbol{r}) = \rho(\boldsymbol{r}) \exp\{\mathrm{i}\chi(\boldsymbol{r})\} = \xi(\boldsymbol{r}) + \mathrm{i}\eta(\boldsymbol{r}) \tag{3}$$

are the intersection points of the nodal lines $\xi = 0$ and $\eta = 0$. If $\psi$ is to be vortex-free, these two sets of nodal lines must avoid each other.

A simple class of vortex-free landscapes is based on the trivial case $\psi = \exp(\mathrm{i}x)$, where $\xi$ has straight nodal lines in the $y$ direction, and those of $\eta$ lie between them. The generalization is to a sum of plane waves in which the absolute value of the coefficient of one exceeds the sum of the absolute values of the coefficients of the others (see [8] for an application of this idea to vortices in three dimensions). All these landscapes are highly anisotropic, in the sense that there is a dominant wavevector $\boldsymbol{k}$. What follows is, by contrast, a construction of vortex-free landscapes where the average $\boldsymbol{k}$ is zero.

To begin, we note that nodal lines of $\xi$ and $\eta$ are of two types: percolating (that is, infinitely long), and closed loops surrounding extrema. For functions that are on the average isotropic, percolating nodal lines will meander back and forth, and it is not easy to imagine any mechanism by which they can avoid each other. Therefore, the construction here is based on $\xi$ and $\eta$ whose nodal lines are all closed loops.

Let $\xi$ be an array of hills located at an arbitrary set of points (not necessarily periodic), with the average height subtracted, to make the mean zero, and let $\eta$ be an array of hills located at a different set of points. If the curvatures of the hilltops are sufficiently large, the nodal lines of $\xi$ and $\eta$ will be loops surrounding each hilltop, and the $\xi$ and $\eta$ loops will not intersect.

In the simplest explicit example, the $\xi$ landscape consists of Gaussian hills centred on the points of a unit square lattice, namely

$$\begin{aligned}\xi(\boldsymbol{r}) &= \frac{1}{\pi a^2} \sum_{m=0}^{\infty} \sum_{n=0}^{\infty} \exp\left\{-\frac{(x-m)^2 + (y-n)^2}{a^2}\right\} - 1 \\ &= 2 \sum_{m=1}^{\infty} (\cos\{2\pi m x\} + \cos\{2\pi m y\}) \exp\{-\pi^2 a^2 m^2\} \\ &\quad + 4 \sum_{m=1}^{\infty} \sum_{n=1}^{\infty} \cos\{2\pi m x\} \cos\{2\pi n y\} \exp\{-\pi^2 a^2 (m^2 + n^2)\} \\ &= \vartheta_3(\pi x, \exp(-\pi^2 a^2)) \vartheta_3(\pi y, \exp(-\pi^2 a^2)) - 1, \end{aligned} \tag{4}$$

where $\vartheta_3$ denotes the elliptic theta function [9], and $\eta$ is the same landscape with the lattice shifted to avoid the $\xi$ hills:

$$\eta(\boldsymbol{r}) = \xi\left(x - \tfrac{1}{2}, y - \tfrac{1}{2}\right). \tag{5}$$

From (4), it is easy to see that the average $\boldsymbol{k}$ is zero.

Figure 1 shows the modulus $|\psi|$, and figure 2 shows the phase contours $\arg\psi$, which have no singularities because the nodal lines of $\xi$ ($\arg\psi = 0$ or $\pi$) do not intersect those of $\eta$ ($\arg\psi = \pm\pi/2$). The closest approaches of the $\xi$ and $\eta$ nodal lines are along the diagonals

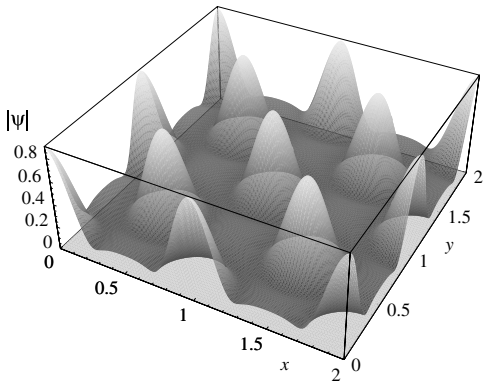


**Figure 1.** Modulus $|\psi(\boldsymbol{r})|$ (equation 3) for four unit cells of the vortex-free Gaussian-hill landscape (4) and (5), with $a = 0.2$.

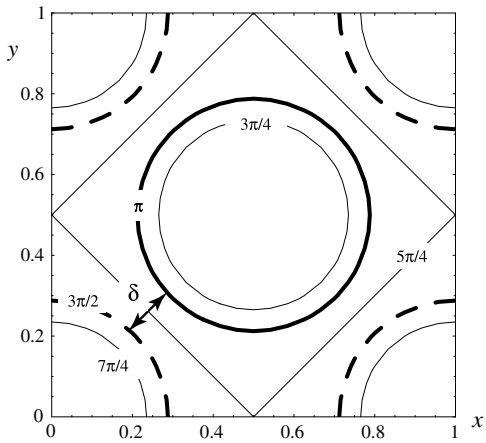


**Figure 2.** As figure 1, showing contours of indicated values of phase $\chi(\boldsymbol{r}) = \arg\psi(\boldsymbol{r})$, with the nodal lines of $\xi$ shown bold, and the nodal lines of $\eta$ shown dashed.

$x = \pm y$, where the separation $\delta$ of the lines (figure 2) decreases from $\frac{1}{\sqrt{2}} - 2a\sqrt{-\log(\pi a^2)}$ for small $a$ (well-separated $\xi$ and $\eta$ hills) to $\frac{\sqrt{2}}{\pi}\exp(-3\pi^2 a^2)$ for large $a$ (nearly overlapping hills).

The phase landscape (contours of $\chi(\boldsymbol{r})$) possesses no vortex singularities, but as a non-trivial smooth function it must have critical points; for each unit cell, these are (figure 2) phase maxima at the corners, phase minima at the centres and phase saddles at the mid-points of the sides.

In this example of Gaussian hills, the $\xi$ and $\eta$ landscapes are not reversible, in the sense that the $\xi$ and $-\xi$ landscapes look different, both statistically or under translation, and similarly for $\eta$ (although both $\xi$ and $\eta$ are, by construction, zero on the average). It seems hard to construct a reversible vortex-free complex landscape where the average $\boldsymbol{k}$ vanishes, but I have not been able to prove that it is impossible.

The vortexless landscape $\psi(\boldsymbol{r})$ (3)–(5) constructed in this section is periodic, and so undulates over the entire $xy$ plane. However, it can easily be modified to represent a beam of

finite extent (for example, optical), for example by multiplying $\psi(\boldsymbol{r})$ by the vortexlessness-preserving Gaussian modulation $\exp(-r^2/2w^2)$.

## 3. Umbilics

For a smooth real scalar function $h(\boldsymbol{r})$, representing the height of a landscape above the $\boldsymbol{r}$ plane, the umbilic points satisfy two equations, which in the limit of small $h$ can be written as

$$\xi_{\mathrm{u}} \equiv h_{xx} - h_{yy} = 0, \qquad \eta_{\mathrm{u}} \equiv 2h_{xy} = 0, \tag{6}$$

where subscripts $x$, $y$ denote derivatives. Thus umbilics are the intersection points of the nodal lines of $\xi_{\mathrm{u}}$ and $\eta_{\mathrm{u}}$.

A possible strategy for creating an umbilic-free landscape is based on the fact that umbilics are locally spherical points: begin with a landscape with many umbilics (in which topology requires equal numbers with indices $+1/2$ and $-1/2$), and then make it anisotropic by stretching in $x$ and squeezing in $y$. However, this is unlikely to succeed, because it is known [6] that for random landscapes even extreme anisotropization only changes the umbilic density (2) by a factor of at most 1.08.

More promising is to note that (6) suggests that the question of the existence of umbilic-free landscapes looks like the question, answered in the affirmative in section 2, of whether vortex-free landscapes exist: the vortices, corresponding to umbilics, can be regarded as zeros $\rho_{\mathrm{u}} = 0$ of the complex scalar function

$$\psi_{\mathrm{u}} = \xi_{\mathrm{u}} + \mathrm{i}\eta_{\mathrm{u}} = \rho_{\mathrm{u}} \exp(\mathrm{i}\chi_{\mathrm{u}}). \tag{7}$$

The analogy is equivalent to a previous idea [10] in which umbilics are regarded as zeros of two-component vectors. It is useful, because the principal curvature directions $\gamma$ and $\gamma + \pi/2$ of the $h$ landscape are given in terms of the phase landscape by $\gamma = \frac{1}{2}\chi_{\mathrm{u}}$.

However, the umbilic problem is harder than the vortex problem, because $\xi_{\mathrm{u}}$ and $\eta_{\mathrm{u}}$ cannot be chosen independently, so their separate nodal lines cannot be freely manoeuvred. From (6), $\xi_{\mathrm{u}}$ and $\eta_{\mathrm{u}}$ are related by

$$2\xi_{\mathrm{u},xy} = \eta_{\mathrm{u},xx} - \eta_{\mathrm{u},yy}. \tag{8}$$

Nevertheless, some freedom remains, and as will now be explained this is sufficient to create umbilic-free functions.

Any landscape can be expressed as a superposition of plane waves with wavevectors $\boldsymbol{k}$, which it is convenient to write in the form

$$h(\boldsymbol{r}) = \sum_{\boldsymbol{k}\neq 0} \frac{c_{\boldsymbol{k}}}{k^2} \cos(\boldsymbol{k}\cdot\boldsymbol{r} - \mu_{\boldsymbol{k}}), \tag{9}$$

with non-negative real coefficients $c_{\boldsymbol{k}}$ and phases $\mu_{\boldsymbol{k}}$. The exclusion $\boldsymbol{k} \neq 0$ ensures that $h$ has zero mean. From (6), the solutions of (8) are

$$\begin{aligned} \xi_{\mathrm{u}}(\boldsymbol{r}) &= \sum_{\boldsymbol{k}\neq 0} c_{\boldsymbol{k}} \cos(2\phi_{\boldsymbol{k}}) \cos(\boldsymbol{k}\cdot\boldsymbol{r} - \mu_{\boldsymbol{k}}) \\ \eta_{\mathrm{u}}(\boldsymbol{r}) &= \sum_{\boldsymbol{k}\neq 0} c_{\boldsymbol{k}} \sin(2\phi_{\boldsymbol{k}}) \cos(\boldsymbol{k}\cdot\boldsymbol{r} - \mu_{\boldsymbol{k}}), \end{aligned} \tag{10}$$

in which $\phi_{\boldsymbol{k}}$ is the polar angle of the wavevector $\boldsymbol{k}$. Relations (10) imply that in $\xi_{\mathrm{u}}$ the contributions from wavevectors near the diagonals $k_x = \pm k_y$ are suppressed, and in $\eta_{\mathrm{u}}$ the contributions near the axes $k_x = 0$ and $k_y = 0$ are suppressed. Therefore $\eta_{\mathrm{u}}$ can be changed without changing $\xi_{\mathrm{u}}$ by changing the coefficients of wavevectors along the diagonal, and $\xi_{\mathrm{u}}$

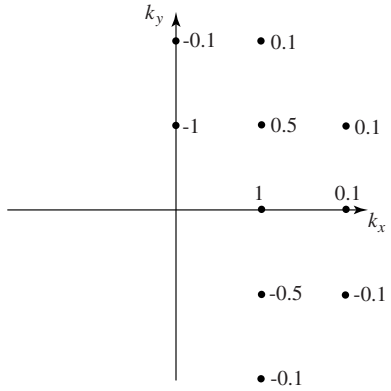


**Figure 3.** Points indicate $\boldsymbol{k}$ vectors in the superposition (9), chosen to represent an umbilic-free landscape, with each vector labelled with its coefficient $\pm c_{\boldsymbol{k}}$ (where the sign indicates whether the phases $\mu_{\boldsymbol{k}}$ are 0 or $\pi$). The $\boldsymbol{k}$ lattice has unit cell size $2\pi$, so that the $h(\boldsymbol{r})$ unit cell has size 1.

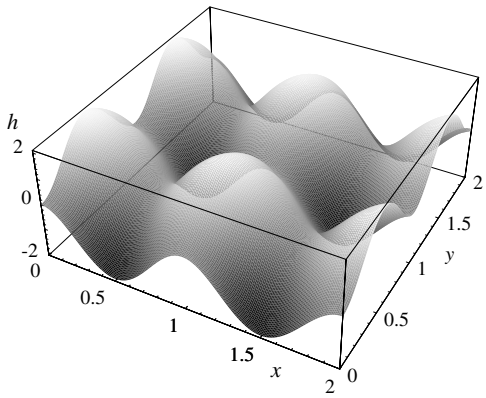


**Figure 4.** Four unit cells of the umbilic-free landscape (9) whose $\boldsymbol{k}$ vectors, coefficients and phases are chosen as in figure 3.

can be changed without changing $\eta_{\mathrm{u}}$ by changing the coefficients of wavevectors along the axes.

By exploiting this observation to guide numerical experiments, I was able to manoeuvre the $\xi_{\mathrm{u}}$ and $\eta_{\mathrm{u}}$ nodal lines away from each other, thereby creating an umbilic-free landscape. This is periodic, with the $\boldsymbol{k}$ vectors and coefficients in (9) chosen as in figure 3. The resulting landscape $h(\boldsymbol{r})$ (figure 4) betrays no sign of its unusual umbilic-free property (which persists under small variations of the coefficients). The nodal lines of $\xi_{\mathrm{u}}$ and $\eta_{\mathrm{u}}$ do not intersect (figure 5), but they come close (for example in the region indicated by the small square) indicating that small perturbations would turn the 'virtual umbilics' into genuine ones.

For an umbilic-free landscape, the two principal curvatures of the landscape are eigenvalues of the Hessian matrix of second derivatives of $h(\boldsymbol{r})$, namely

$$C_{\pm} = \tfrac{1}{2}\big(\nabla^2 h \pm \sqrt{\xi_{\mathrm{u}}^2 + \eta_{\mathrm{u}}^2}\big). \tag{11}$$

In the usual case, when there are umbilics, the surfaces representing these curvatures meet at diabolical points [11], that is conical intersections. For umbilic-free surfaces, they never meet,

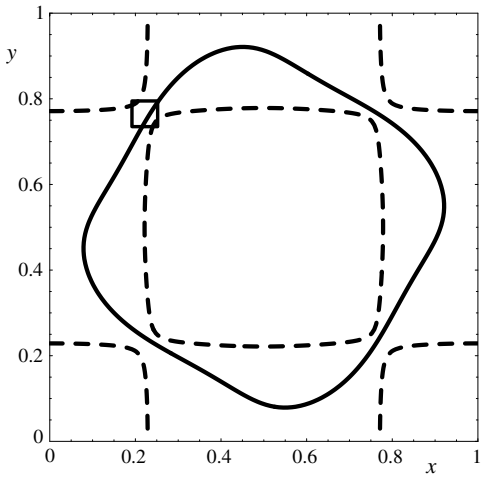


**Figure 5.** As figure 4, showing nonintersecting nodal lines of $\xi_u(\boldsymbol{r})$ (full curve) and $\eta_u(\boldsymbol{r})$ (dashed curves) as in (10). The small square includes one of the four regions where the nodal lines almost intersect, i.e. where the two principal curvatures are almost equal.

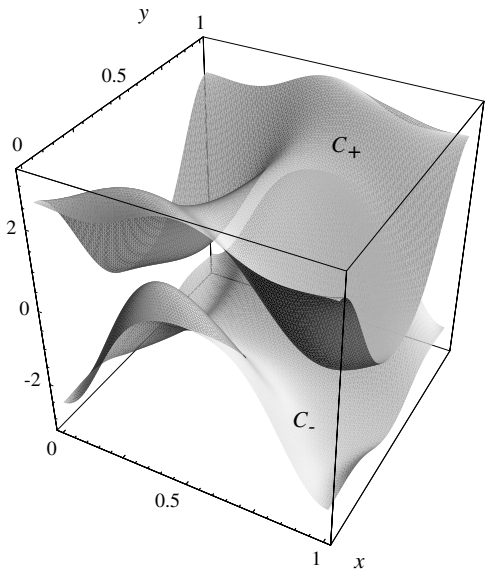


**Figure 6.** Principal curvatures $C_\pm$ (equation 11) corresponding to the umbilic-free landscape of figure 4.

as illustrated in figure 6. The net of orthogonal curvature directions, calculated as described after (7), is shown in figure 7. From the magnifications shown, it is clear that there are none of the index $\pm 1/2$ star, lemon or monstar singularities [6] associated with umbilic points, but the intricate swirling pattern of curvature lines indicates the near-birth of a pair of virtual umbilics, that would become real if the coefficients in figure 3 were changed slightly.

If the surface $h(\boldsymbol{r})$ represents a wavefront, the loci at points defined by distances $1/C_+$ and $1/C_-$ along the normals are the two caustic surfaces (envelope of normals) [3]. Usually

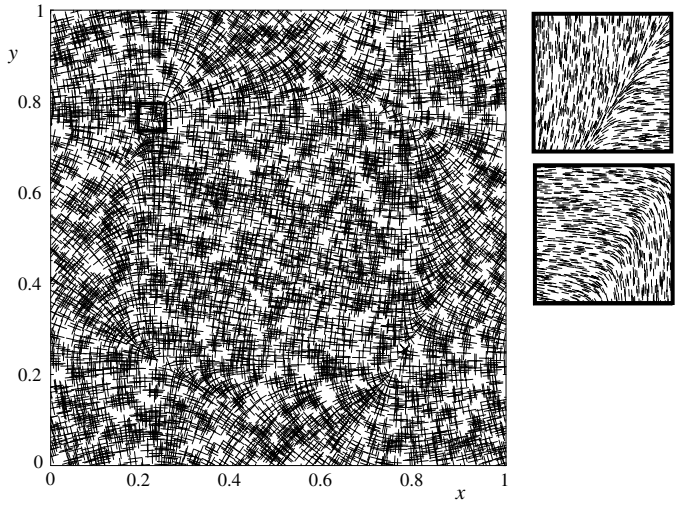


**Figure 7.** Orthogonal net of principal curvature directions on the umbilic-free landscape of figure 4, with the small square as in figure 5. The pictures on the right are magnifications of the directions of the two separate curvatures within the small square, showing that the patterns of curvature directions are non-singular.

these meet, at elliptic or hyperbolic umbilic foci, situated along the normals from umbilic points on the surface. For an umbilic-free wavefront, this cannot happen, and the only generic singularities on each otherwise smooth (fold) caustic surface are cusp lines, where the surface is ribbed.

## 4. Concluding remarks

It is clear that these vortex-free and umbilic-free landscapes are exceptional, but this seems hard to quantify. One possible way to calculate the measure of the exceptional landscapes is to consider the class of landscapes represented by a sum of $N$ plane waves whose amplitudes and wavevectors are fixed, and with a zero mean wavevector, and calculate the probability $P$ of there being no vortices or umbilics by averaging over the phases. This is

$$P = \left\langle \delta \left[ \iint \mathrm{d}^2\boldsymbol{r}\, \delta(\xi(\boldsymbol{r}))\delta(\eta(\boldsymbol{r})) \left| \det\left( \frac{\delta(\xi,\eta)}{\delta(x,y)} \right) \right| \right] \right\rangle, \tag{12}$$

where for vortices $\xi$ and $\eta$ are arbitrary $N$-wave superpositions, and have the form (10) for umbilics.

Precise calculation seems hard, even when $N$ is not large. I conjecture that $P$ falls rapidly to zero as $N$ increases.

## Acknowledgments

I thank Mark Dennis, John Hannay and John Nye for helpful conversations, and Marat Soskin for the question (Must every hilly landscape possess umbilics?) that stimulated this work. My research is supported by the Royal Society of London and the University of Bristol.

## References

[1] Berry M V and Upstill C 1980 Catastrophe optics: morphologies of caustics and their diffraction patterns *Prog. Opt.* **18** 257–346
[2] Berry M V 1981 *Singularities in waves and rays Les Houches Lecture Series Session* vol 35 ed R Balian, M Kléman and J-P Poirier (Amsterdam: North-Holland) pp 453–543
[3] Nye J F 1999 *Natural Focusing and Fine Structure of Light: Caustics and Wave Dislocations* (Bristol: Institute of Physics Publishing)
[4] Nye J F and Berry M V 1974 Dislocations in wave trains *Proc. R. Soc.* A **336** 165–90
[5] Porteous I 1994 *Geometric Differentiation: for the Intelligence of Curves and Surfaces* (Cambridge: Cambridge University Press)
[6] Berry M V and Hannay J H 1977 Umbilic points on Gaussian random surfaces *J. Phys. A: Math. Gen.* **10** 1809–21
[7] Berry M V and Dennis M R 2000 Phase singularities in isotropic random waves *Proc. R. Soc.* A **456** 2059–9
[8] O'Holleran K, Padgett M J and Dennis M R 2006 Topology of optical vortex lines formed by the interference of three, four, and five plane waves *Opt. Express* **14** 3039–44
[9] Abramowitz M and Stegun I A 1972 *Handbook of Mathematical Functions* (Washington: National Bureau of Standards)
[10] Dennis M R 2003 Correlations and screening of topological charges in Gaussian random fields *J. Phys. A: Math. Gen.* **36** 6611–28
[11] Berry M V and Wilkinson M 1984 Diabolical points in the spectra of triangles *Proc.R. Soc.* A **392** 15–43